

kinetic-energy" model is given by D. J. Thouless, *The Quantum Mechanics of Many-Body Systems* (Academic, New York, 1961), p. 101.

<sup>11</sup>L. P. Gorkov, *Zh. Eksp. Teor. Fiz.* **34**, 735 (1958) [*Sov. Phys. JETP* **34**, 505 (1958)].

<sup>12</sup>W. A. Little, *Phys. Rev.* **134**, A1416 (1964).

<sup>13</sup>R. A. Bari, *Phys. Rev. B* **3**, 2662 (1971).

<sup>14</sup>A straightforward application of molecular-field theory in the presence of two order parameters gives the free energy (per site)  $f = \Delta^2/4I_2 + \delta^2/4I_3 - kT \ln\{2[e^{\beta I_1/2} + \cosh[\frac{1}{2}\beta(\Delta^2 + \delta^2)^{1/2}]]\}$  where  $\delta$  represents the order parameter of the ferroelectric phase. We also note that the

competition between a lattice distortion and superconductivity had been studied in the opposite limit of the Hubbard model ( $I_1=0$ ,  $t_{ij} \neq 0$ ) by D. C. Mattis and W. D. Langer, *Phys. Rev. Letters* **25**, 376 (1970).

<sup>15</sup>P. W. Anderson, *Phys. Rev.* **112**, 1900 (1958).

<sup>16</sup>P. M. Chaikin, A. F. Garito, and A. J. Heeger, *Phys. Rev. B* **5**, 4966 (1972).

<sup>17</sup>Yu. A. Bychkov, L. P. Gorkov, and I. E. Dzyaloshinskii, *Zh. Eksp. Teor. Fiz.* **50**, 738 (1966) [*Sov. Phys. JETP* **23**, 489 (1966)]; I. E. Dzyaloshinskii and A. I. Larkin, *Zh. Eksp. Teor. Fiz.* **61**, 791 (1971) [*Sov. Phys. JETP* **34**, 422 (1972)].

## Transferred Magnetically Induced $\text{Al}^{27}$ Quadrupole Interaction in $\text{GdAl}_2$

J. Degani\* and N. Kaplan

*The Racah Institute of Physics, The Hebrew University, Jerusalem, Israel*

(Received 15 August 1972)

A direct observation of a magnetically induced electric field gradient (efg) at a *nonmagnetic* Al site in ferromagnetic  $\text{GdAl}_2$  is described. The efg was determined from accurate measurements of the  $\text{Al}^{27}$  nuclear-spin-echo envelope-modulation frequency, performed on Al in *a* sites for which the magnetization  $\vec{M}$  and the crystalline efg axis are colinear. Monitored as function of  $M$ , it is found that the total efg in *a* sites is given by  $q = q_c - (M/M_{\text{sat}})q_m$ , with  $e^2 Q^{27} q_c = 4.19 \pm 0.05$  MHz and  $e^2 Q^{27} q_m = 0.577 \pm 0.05$  MHz. The origin of  $q_m$  is as yet unclear, since simple models leading to induced efg will result in  $M^2$  dependence for the transferred induced efg term, contrary to the linear  $M$  dependence presently observed.

In recent years there have been several reports about nuclear-quadrupole-interaction (QI) measurements in which a magnetically induced electric field gradient (efg) was observed at the nuclear site of magnetic ions in solids.<sup>1,2</sup> In these ions the electronic wave functions of the unfilled magnetic shell, and thus the charge distribution around the ionic nucleus, depend on the state of magnetization of the ion, which in turn results in a magnetization-dependent efg. Now, in analogy with the case of magnetic hyperfine interactions, one might also search for a process in which the efg at the nuclear site of *nonmagnetic* ions in a crystal is effected by the state of magnetization of a *neighboring* magnetic ion. In principle, any crystal in which magnetic-transferred hyperfine interaction has been identified is suitable for such a search provided  $I \geq 1$ , where  $I$  is the spin of the nucleus of the nonmagnetic ions. The search to be described was conducted on ferromagnetic  $\text{GdAl}_2$ , in which the Gd has the role of the magnetic ions and the sizable  $M$ -dependent  $\text{Al}^{27}$  QI was detected in the nonmagnetic Al ions. We believe this report provides the first direct experimental evidence for the existence of a transferred magnetically induced efg in solids.<sup>3</sup>

Familiarity with some features of the compound is essential for the understanding of the present

experiment:  $\text{GdAl}_2$  is an intermetallic compound of the cubic Laves phases structure<sup>4</sup>; there are 16 Al ions in the cubic cell (Fig. 1), forming four tetrahedra, and the point symmetry of each Al is  $\bar{3}m$ , with the threefold symmetry axes parallel to the principal diagonals of the cubic unit cell; below 176°K, the Gd moments order ferromagnetically

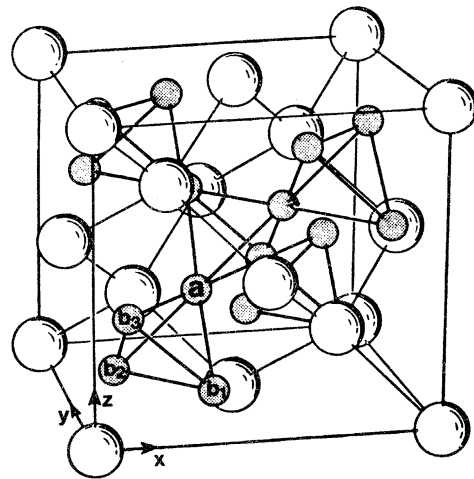


FIG. 1. Unit cell of  $\text{GdAl}_2$ . Large circles represent Gd and small shaded circles represent Al ions.

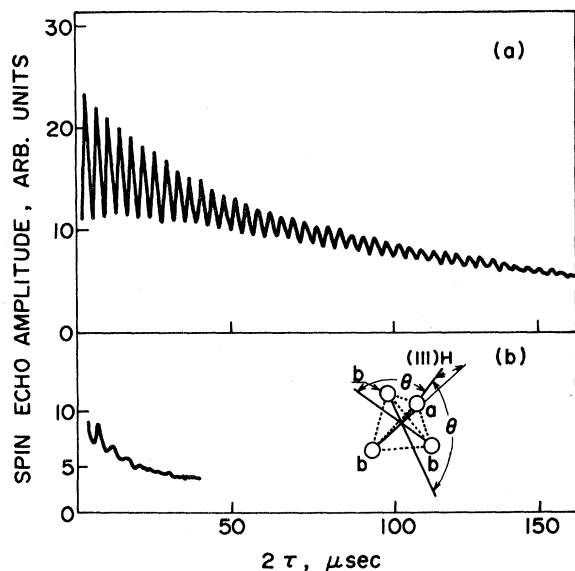


FIG. 2. Spin-echo-decay modulations at 80°K. (a) Observation on  $a$  sites; (b) Observation on  $b$  sites. Insert in (b) shows the geometry of an Al tetrahedron.

along the  $[111]$  direction,<sup>5,6</sup> forming two inequivalent Al-site groups—representatives of which are labeled (a) and (b) in Fig. 1. The  $\text{Al}^{27}$  Hamiltonians of the groups differ from each other. First, the local magnetic field acting on  $\text{Al}^{27}$  in  $a$  sites is  $\sim 20\%$  larger than that acting on  $\text{Al}^{27}$  in  $b$  sites, resulting in two well-separated NMR absorption lines,  $a$  and  $b$ , which can be studied separately. Secondly, the direction of the threefold symmetry axis passing through an  $a$  site coincides with the  $[111]$  direction of  $\vec{M}$ , whereas the threefold axes through the  $b$  site, directed along  $[1\bar{1}1]$ ,  $[1\bar{1}\bar{1}]$ , and  $[1\bar{1}\bar{1}]$ , form an angle  $\theta = 70^\circ 32'$  with the  $[111]$  direction of  $\vec{M}$  [see insert in Fig. 2(b)]. We shall return to the symmetry problem later in the paper.

The QI in the present study was measured by utilizing a spin-echo technique first described by Abe, Yasuoka, and Hirai.<sup>7</sup> The method can be outlined briefly as follows: When a QI term is added to a nuclear Zeeman Hamiltonian, the usual monotonic  $T_2$  decay of the nuclear-spin-echo envelope, following a standard  $\frac{1}{2}\pi - \tau - \pi$  pulse sequence, is modulated by oscillations, the frequency of which depends on the QI. For an axially symmetric efg, the explicit expression given in Ref. 7 for the echo amplitude, for nuclei with  $I = \frac{5}{2}$  (as in  $\text{Al}^{27}$ ), is

$$E(2\tau) = e^{-2\tau/T_2} \sum_{n=0}^4 C_n \cos(2na\tau + \delta_n) \quad (1)$$

where  $a = [3e^2Q^{27}q/8I(2I-1)](3\cos^2\theta - 1)$ ,  $C_n$  and  $\delta_n$  are constants depending on initial conditions and on the shape and width of the rf pulses, and  $\theta$  is

the angle between the efg axis and the local magnetic field. It has been found in the course of the present study that for practical purposes the higher harmonic terms in (1) can be neglected. We then write

$$E(2\tau) = e^{-2\tau/T_2} [C_0 + C_1 \cos(2a\tau + \delta_1)] \quad (2)$$

with  $T_2$ ,  $\delta_1$ ,  $C_1/C_0$ , and  $a$  as parameters, and it is immediately verified that the echo decay is indeed modulated at a frequency proportional to the QI.

Using a rather elaborate signal-averaging system, we have recorded accurately—both digitally and graphically—the modulated-echo-decay envelope as a function of the separation  $\tau$  between the rf pulses. A representative graphical recording, obtained by accumulating data during a  $\sim 10$ -min period for  $a$ -site nuclei at 80°K, is shown in Fig. 2(a). A least-square fitting of the theoretical functional decay (2) to the experimentally recorded data yields immediately the value of  $a$ , with typical accuracy of  $\pm 0.3\%$ . In favorable cases, e.g., when temperature errors were minimal, accuracies as high as  $\pm 0.006\%$  were realized. The accuracy obtained for the QI is remarkable if one notes that the NMR width of the  $a$  absorption line, as well as that of the  $b$  line, is  $\sim 4$  MHz.<sup>5,6</sup> This broadening reflects a spread in the total Hamiltonian of individual  $a$  sites which is 3 to 4 orders of magnitude larger than the typical error quoted above for the QI, and it demonstrates the power of the present technique to uncover relatively small QI, otherwise masked by much larger Zeeman inhomogeneity.

Technique and accuracy at hand, it is a simple matter of measuring the echo-decay modulation as function of  $M$ , from which  $a(M)$  is readily determined as above. The variation of  $M$ , in the range  $0.59 \leq M/M_{\text{sat}} \leq 0.99$ , was achieved by varying sample temperature between 4 and 112°K, with  $M$  values being determined from two independent experimental  $M(T)$  curves.<sup>8,9</sup> The resulting variation of  $3e^2Q^{27}q/4I(2I-1)$  with  $M$  for the  $a$  group—for which  $\theta = 0^\circ$ —is shown in Fig. 3, where the remarkable linear decrease of the QI with increasing  $M$  is clearly displayed, providing direct evidence for the existence of transferred magnetically induced efg at the  $a$  sites of  $\text{GdAl}_2$ . Similar measurements were conducted also on  $b$  nuclei and a typical recording, again accumulated during  $\sim 10$ -min period at 80°K, is shown in Fig. 2(b). The accuracy in determining modulation frequencies  $f$  on  $b$  sites is much poorer than that for  $a$  sites, but once again a significant  $M$  dependence could be detected in  $f$ .

Marked differences between the results observed for the two site groups deserve further attention: (i)  $f$  observed for  $b$  sites [Fig. 2(b)] is only about

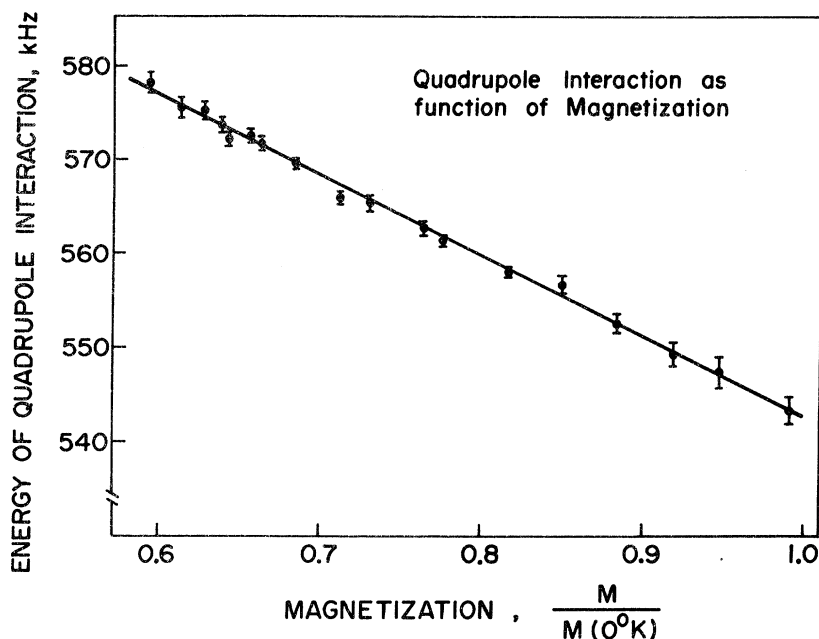


FIG. 3. Dependence of  $3e^2Qq/4I(2I-1)$  on  $M$  for  $a$  sites.

one-half that of  $f(a)$  [e. g.,  $f(b) = 280 \pm 3$  kHz at  $77^\circ\text{K}$ ]; (ii) the "quality factor" of the modulation, defined as the number of observable oscillations divided by  $f$ , is about 10 times larger for  $a$  signals than for  $b$  signals; (iii) the "quality factor" of the  $b$  line deteriorates substantially as  $M$  decreases, whereas that of the  $a$  line remains essentially constant. A closer look at the environment of each site is required to explain the differences. The general nuclear Hamiltonian, including both Zeeman and quadrupole interactions, is given exactly by

$$\mathcal{H} = \gamma h H_0 I_z + \frac{e^2 Q q}{4I(2I-1)} [3I_z^2 - I(I+1) + \frac{1}{2} \eta (I_+^2 - I_-^2)], \quad (3)$$

where the  $(x, y, z)$  coordinates are selected so that  $H_0$  is along the  $z$  axis and the spin components  $I_z$ ,  $I_+$ , and  $I_-$  are expressed in the principal coordinate system  $(X, Y, Z)$  of the efg tensor  $V_{ij} = \partial^2 V / \partial x_i \partial x_j$ . In general the  $z$  direction does not coincide with any of the  $X, Y, Z$  axes. The Hamiltonian (3) can now be written explicitly for the  $\text{Al}^{27}$  in  $\text{GdAl}_2$  after assuming that there are two sources for the efg; the first is the usual crystalline efg, which is the only source in paramagnetic  $\text{GdAl}_2$ . As each Al has a threefold crystallographic axis, the crystalline efg,  $q_c$ , has also a symmetry axis, parallel to the crystallographic one. A second source is a magnetically induced efg,  $q_m(M)$ . Obviously,  $q_m$  must be axially symmetric along the  $\vec{M}$  direction, namely, along  $[111]$ , for both site groups. Thus, the two groups will possess different symmetry properties and must be treated separately.

*Group a.* Here the direction of  $\vec{M}$  (which is also

the direction of the local magnetic field) coincides with the crystallographic axis, both being along  $[111]$ , and as a result both  $q_c$  and  $q_m(M)$  have the same axial-symmetry direction. Therefore the total efg will be axially symmetric (i. e.,  $\eta = 0$ ) along the local magnetic field (i. e.,  $\vec{z} \parallel \vec{z}$ ). In this case the Hamiltonian (3) can be considerably simplified and we can write

$$\mathcal{H}(a) = \gamma h H_0(a) I_z + \frac{e^2 Q q}{4I(2I-1)} [3I_z^2 - I(I+1)]. \quad (4)$$

The Hamiltonian (4) is diagonal and the transition frequency  $\Delta\omega_n$  between two adjacent energy states  $E_n$  and  $E_{n-1}$  will be given simply by

$$\Delta\omega_n \equiv \frac{E_n - E_{n-1}}{h} = \gamma H_0 + (2n-1) \frac{3e^2 Q q}{4I(2I+1)}; \quad (5)$$

$$n = I, \dots, -|I-1|.$$

When transitions between several  $n \rightarrow n-1$  pairs are induced simultaneously—as is the case in the present spin-echo study—the interference between adjacent transitions results in a beat, or modulation of the average transition frequency, given by

$$\omega_{\text{mod}} = \frac{1}{2} (\Delta\omega_n - \Delta\omega_{n-1}) = \frac{3e^2 Q q}{4I(2I-1)}. \quad (6)$$

We therefore expect the echo decay of  $a$  sites to be modulated in accord with (6), but  $\omega_{\text{mod}}$ , as given in (6), is indeed identical with the modulation frequency  $a$  found by Abe *et al.* in their calculation. Because  $\omega_{\text{mod}}$  in (6) is the same for every two adjacent transitions, beats from all the transition pairs interfere constructively, resulting in

the large "quality factor" that was observed for the *a* line. From (5) and (6) it is also apparent that the modulation frequencies listed in Fig. 3 are proportional to the efg  $q$ , and the proportionality coefficient is independent of  $M$ . Thus, in group *a* the variation of the modulation frequency is a direct measure to the variation of the efg.

*Group b.* Here the situation is different. While  $q_c$  and  $q_m$  each have axial symmetry, the two axes are in different directions. The total efg tensor therefore lacks any special symmetry, and in the ( $X$ ,  $Y$ ,  $Z$ ) system the local magnetic field will be in some general direction  $\Omega(\theta, \phi)$ . As the Zeeman interaction ( $\sim 50$  MHz) is much larger than the QI ( $\sim 4$  MHz) it is convenient to choose quantization direction  $z$  along the local field  $H_0$ . Transforming from the ( $X$ ,  $Y$ ,  $Z$ ) system results in a general *nondiagonal* Hamiltonian  $\mathcal{H}(b) = \mathcal{H}^1(b) + \mathcal{H}^2(b) + \dots$ . The first-order term is given by

$$\mathcal{H}^1(b) = -\gamma h H_0(b) I_z + \frac{e^2 Q q}{8I(2I-1)} G [3I_z^2 - I(I+1)], \quad (7)$$

where  $G = 3 \cos^2 \theta - 1 + \eta \sin^2 \theta \cos 2\phi$ . The size of the higher-order terms depends on the ratio of  $e^2 Q q / h \gamma H_0 = \nu_Q / \nu_M$ . For  $\nu_Q / \nu_M \ll 1$ , the diagonal term (7) would describe the system and, as in the *a* group, we should observe modulation  $f(b) = [3e^2 Q q / 8I(2I-1)] G$ , with a large "quality factor." For larger  $\nu_Q / \nu_M$  the nondiagonal terms  $\mathcal{H}^2(b) + \dots$  become important and the beat frequency of the different adjacent transition pairs will differ from each other, resulting in four different  $\omega_{\text{mod}}$  [unlike the situation described in (6)]. A destructive interference will result and the "quality factor" will deteriorate with increasing  $\nu_Q / \nu_M$ . Since for the present study  $\nu_Q / \nu_M \approx 0.08$  at 4.2 °K, and the ratio increases as  $M$  decreases ( $\nu_M$  becomes smaller), both the poor quality factor and the deterioration of it with decreasing  $M$ , which have been observed for the *b* line, are to be expected. Furthermore, from (7) it is evident that even if higher-order terms are negligible, modulation of *b* is still proportional to  $G$ , and  $M$  dependence of  $G$  may be

caused by any of the parameters  $q, \eta, \theta, \phi$ , apart from the direct  $M$  dependence of  $q$ . We conclude that presently only line *a* is suitable for a reliable measure of the induced efg, and consequently the method used in Ref. 5 to deduce the existence of measurable  $q_m$  was insufficient for that purpose.

Returning to the QI data of line *a*, the total efg parameter  $q$  is best described as

$$q = q_c - \frac{M}{M_{\text{sat}}} q_m, \quad e^2 Q q_c = 4.19 \pm 0.05 \text{ MHz}, \\ e^2 Q q_m = 0.577 \pm 0.05 \text{ MHz}. \quad (8)$$

It is reassuring to note that the value of the crystalline efg  $q_c$  in (8) is in excellent agreement with measurements made in paramagnetic GdAl<sub>2</sub>.<sup>10</sup> We conclude from (8) that there is a negative magnetically induced efg on the Al<sup>27</sup> of *a* sites, opposite in sign to  $q_c$ , which depends linearly on  $M$ .

The exact origin for  $q_m$  is not yet understood. One could suggest mechanisms leading to induced efg, such as (i) direct exchange interaction between the tail end of the Gd 4*f* wave functions and the partially localized 3*p*, or even inner 2*p*, electrons of the Al. This interaction will unquench the 3*p* and 2*p* orbitals through the spin-orbit coupling, and thus will redistribute electron charges around the Al<sup>27</sup>; (ii) indirect process in which conduction electron is first exchange polarized by the 4*f* shell and then exchange interacts further with the Al *p* electrons, the rest being the same as in mechanism (i). However, simple arguments lead to the conclusion that both of the above mechanisms would lead to  $M^2$  dependence of the induced efg, contrary to the experimental results. It is believed that similar measurements in single-crystal GdAl<sub>2</sub> and on some other RAl<sub>2</sub> ( $R$  is a rare earth) compounds would be required before the dominant mechanism causing the induced efg will be clearly identified.

Discussions with M. Weger, S. Alexander, and A. J. Freeman and the skillful help of H. Boasson with the necessary electronics are gratefully acknowledged.

\*Supported by a Fellowship from the Israel National Council for Research and Development.

<sup>1</sup>U. Ganiel and S. Shtrikman, Phys. Rev. **167**, 258 (1968).

<sup>2</sup>J. Gal, Z. Hadari, E. R. Bauminger, I. Nowik, S. Ofer, and M. Perkel, Phys. Lett. A **31**, 511 (1970).

<sup>3</sup>It will be shown in the present report that claims made previously in Ref. 5 concerning the observation of induced efg were not sufficiently founded.

<sup>4</sup>J. H. Wernick and S. Geller, Trans. Metall. Soc. AIME **218**, 806 (1960).

<sup>5</sup>N. Shamir, N. Kaplan, and J. H. Wernick, J. Phys. (Paris)

**32**, C1-902 (1971).

<sup>6</sup>N. Kaplan, E. Dormann, K. H. J. Buschow, and D. Lebenbaum, Phys. Rev. B (to be published).

<sup>7</sup>H. Abe, H. Yasuoka, and A. Hirai, J. Phys. Soc. Jap. **21**, 77 (1966).

<sup>8</sup>H. J. Williams, J. H. Wernick, E. A. Nesbitt, and R. C. Sherwood, J. Phys. Soc. Jap. **17**, 191 (1962).

<sup>9</sup>N. Shamir, M. Sc. thesis (The Hebrew University, 1970) (unpublished).

<sup>10</sup>E. D. Jones and J. E. Budnick, J. Appl. Phys. **37**, 1250 (1966).